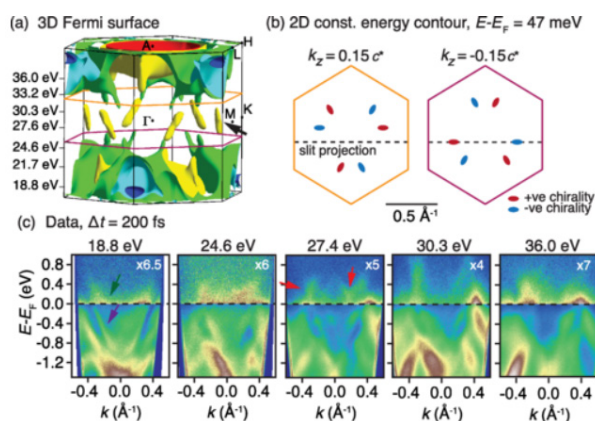


Imaging and Dynamics for Physical and Life Sciences

Ultrafast carrier dynamics throughout the three-dimensional Brillouin zone of the Weyl semimetal PtBi₂

Using time- and angle-resolved photoemission spectroscopy, we examine the unoccupied electronic structure and electron dynamics of the type-I Weyl semimetal PtBi₂. Using the ability to change the probe photon energy over a wide range, we identify the predicted Weyl points in the unoccupied three-dimensional band structure and we discuss the effect of k_{\perp} broadening in the normally unoccupied states. We characterise the electron dynamics close to the Weyl point and in other parts of three-dimensional Brillouin zone using k -means, an unsupervised machine learning technique. This reveals distinct differences—in particular, dynamics that are faster in the parts of the Brillouin zone that host most of the bulk Fermi surface than in parts close to the Weyl points.



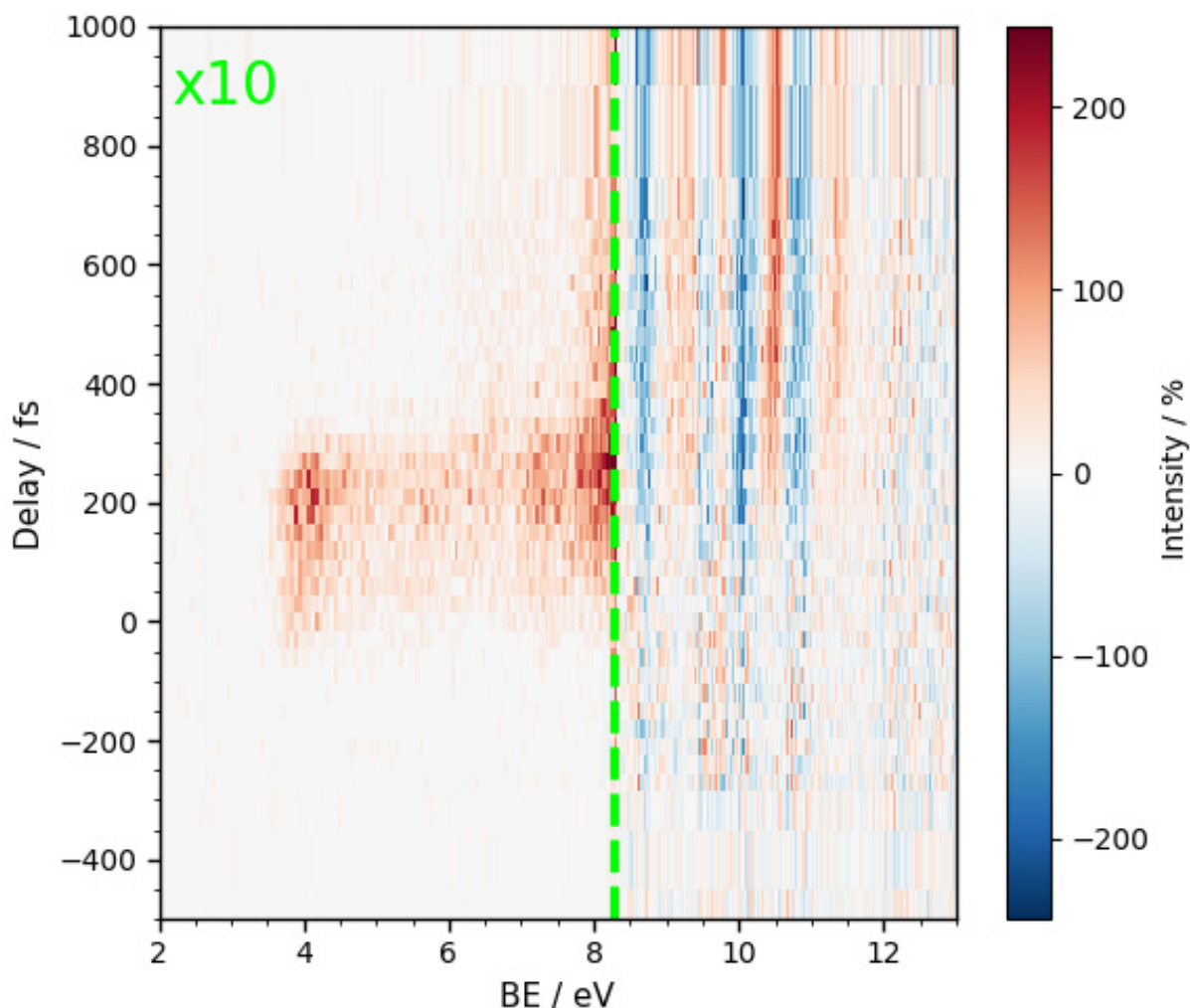
(a) Bulk Brillouin zone and Fermi surface of PtBi₂. The k_z values for the photon energies in our experiment are marked, as well as the planes containing the Weyl points. (b) Two-dimensional cuts through the Brillouin zone at k_z indicated by the corresponding colours in panel (a). The dashed line shows the approximate location of the reported ARPES measurements. The markers represent the location of the Weyl points and the colour their chirality. (c) Dispersion along this dashed line in panel (b) for different probe photon energies following pumping by a 1.46 eV laser pulse at peak excitation. A different grey scale is chosen for the states below and above the Fermi energy, as indicated by insets. Teal (purple) arrows point to the metallic bulk (surface) states.

Subsequently published by the American Physical Society in Machine-learning approach to understanding ultrafast carrier dynamics in the three-dimensional Brillouin zone of PtBi₂, Phys. Rev. Research 7, 013025 (2025) under the terms of the **CC-BY-4.0 license**. doi: 10.1103/PhysRevResearch.7.013025

Authors: P. Majchrzak, C. Sanders, Y. Zhang, A. Kuibarov, O. Suvorov, E. Springate, I. Kovalchuk, S. Aswartham, G. Shipunov, B. Büchner, A. Yaresko, S. Borisenko, **P. Hofmann** ✉

Time-resolved photoelectron spectroscopy study of halothiophene photochemistry

Halothiophenes are heterocyclic rings containing a sulphur (S) atom, with a penderal halogen attached. The photochemistry is highly dependent on the character of both the halogen attached, and the character of the initially excited state. We have compared the photochemistry of bromo and iodothiophene at two pump wavelengths and see wavelength and halogen dependent changes in the photochemistry. In this article we report on the iodothiophene photochemistry occurring upon excitation of the $\pi\pi^*$ or $(n/\pi)\sigma^*$ states.

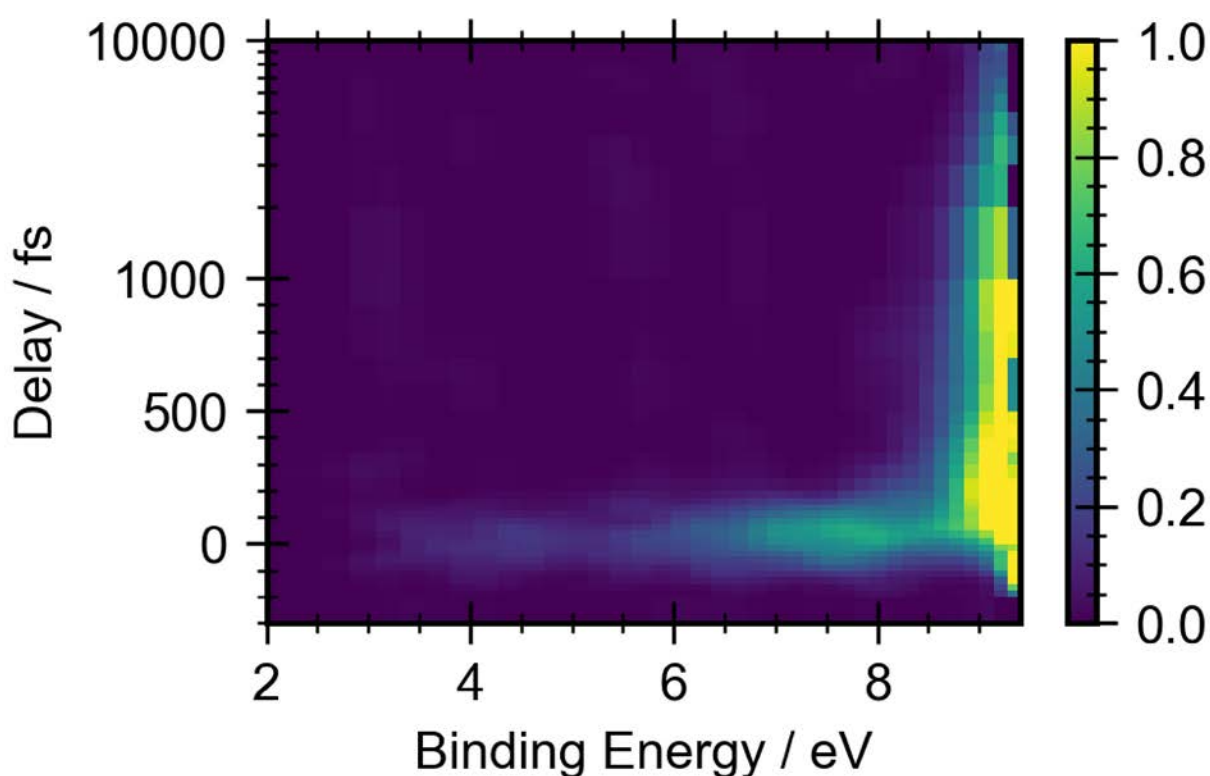


Time-resolved photoelectron spectra of UV (245 nm) pumped 2-iodothiophene. Structural changes are seen as shifts in binding energy as a function of time with iodine and thiophenyl radical product formation seen with a few hundred femtoseconds.

Authors: W.O. Razmus, H.J. Thompson, **R.S. Minns** ✉, M.A. Parkes, E. Springate, R.T. Chapman, Y. Zhang, J.O.F. Thompson

Ultrafast dynamics in the 1,2-dichloroethenes

Isomerisation is a crucial process that occurs following absorption of a photon, it is especially prevalent for C=C double bonds. Isomerisation around a carbon double bond being at the root of vision. It is therefore important to look at how different isomers of different molecules behave. Using a 200 nm pump and an XUV (22 eV probe) we looked at the time resolved photoelectron signals from *trans* and *cis*-1,2-dichloroethene. The position of the signals in the photoelectron spectrum indicates what products are being formed. We observe an ultrafast decay from the initially formed molecular excited state to the ground state. This decay is slower in the *trans* isomer compared to the *cis*. This shows the effect of the relative position of the chlorine atoms. Rapid formation of fragments was also observed on an ultrafast timescale, showing how quickly dissociation can occur.



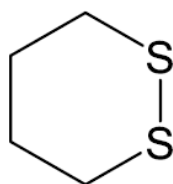
Pump-Probe photoelectron spectrum of *trans*-1,2-dichloroethene with 200 nm pump, 22 eV probe.

Subsequently published in Phys. Chem. Chem. Phys., 26, 28406 (2024) under the terms of the **CC-BY-3.0 license**. doi: 10.1039/d4cp02952f

Authors: H.G. McGhee, H.J. Thompson, J. Thompson, Y. Zhang, A.S. Wyatt, E. Springate, R.T. Chapman, D.A. Horke, R.S. Minns, R.A. Ingle, **M.A. Parkes** ✉

Ring-opening dynamics of a cyclic disulfide captured by time-resolved Coulomb explosion imaging

We used Coulomb explosion imaging, an ultrafast time resolved structure determination technique, to show how the molecular structure of 1,2-dithiane, a model cyclic disulfide, evolves when the disulfide bond is broken with ultraviolet light. Our preliminary analysis reveals that breaking the disulfide bond on the first excited state creates a vibrational wavepacket that represents a torsional motion of the molecular structure, oscillating between a closed and linear biradical structure on a period of approximately 400 femtoseconds. This is in direct agreement with quantum dynamics simulations and this vibrational wavepacket dynamics is observable in our experimental fragment ion yields. We rationalise our observation by calculating how the first, second and third ionisation potentials of 1,2-dithiane vary as the molecular geometry evolves along this vibrational motion. Our work shows how disulfide bonds respond to ultraviolet radiation. They provide an empirical validation of theoretical quantum dynamics calculations and demonstrate the suitability of 1,2-dithiane as a powerful benchmark molecule for ultrafast structural dynamics techniques.



1,2-dithiane ($C_4H_8S_2$)

Figure 1: The molecular structure of 1,2-dithiane.

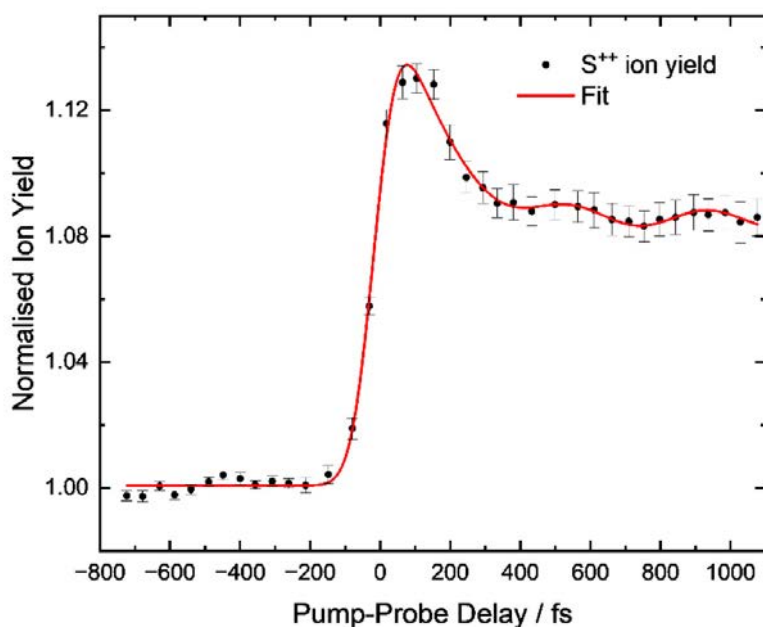


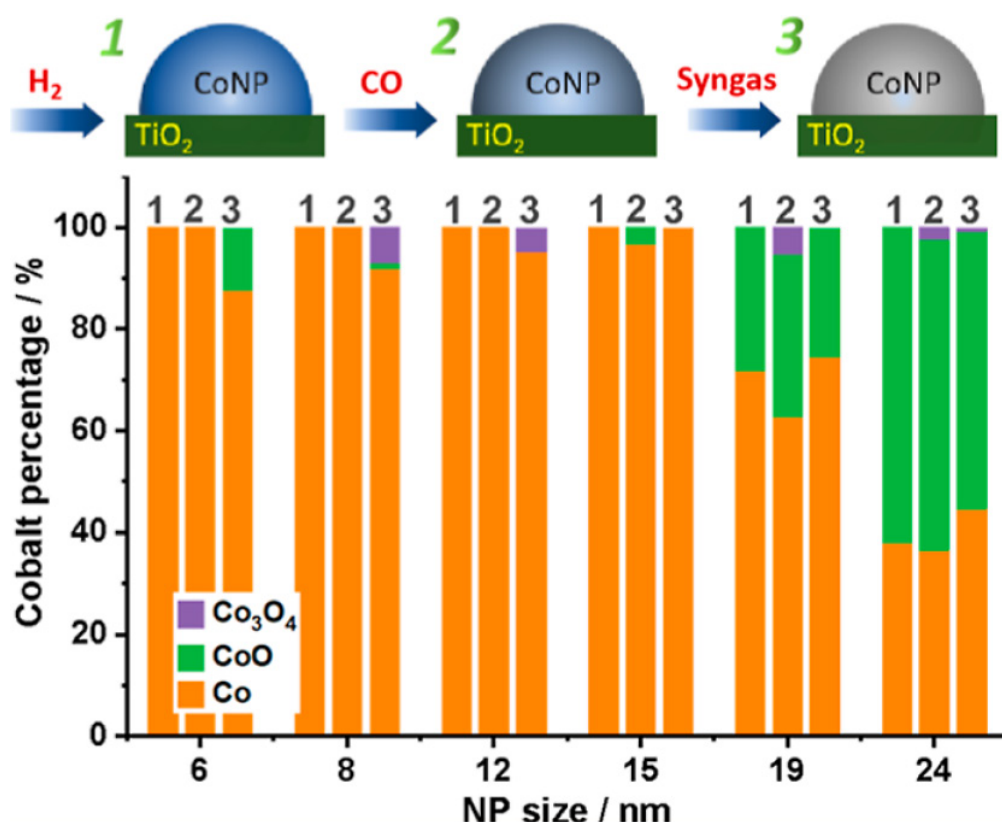
Figure 2: Time-dependent S^{++} ion yield from the Coulomb explosion of 1,2-dithiane following UV photoexcitation.

Subsequently published in Chemical Physical Letters, 871, 142095 (2025) under the terms of the **CC-BY-4.0 license**. doi: 10.1016/j.cplett.2025.142095

Authors: P.A. Robertson ✉, J. Merrick, D. Heathcote, M.S. Robinson, A.A. Butler, J.F.P. Nunes, C. Rankine, Z. Liu, S. Arrowsmith, J.O.F. Thompson, N.M. Madugula, Y. Zhang, R. Chapman, E. Springate, Y. Biddick, E.A. Anderson, A. Kirrander, C. Vallance

Compositional evolution of individual CoNPs on Co/TiO₂ during CO and syngas treatment resolved through soft XAS/X-PEEM

The nanoparticle (NP) redox state is an important parameter in the performance of cobalt-based Fischer–Tropsch synthesis (FTS) catalysts. Here, the compositional evolution of individual CoNPs (6–24 nm) in terms of the oxide vs metallic state was investigated in situ during CO/syngas treatment using spatially resolved X-ray absorption spectroscopy (XAS)/X-ray photoemission electron microscopy (X-PEEM). It was observed that in the presence of CO, smaller CoNPs (i.e., ≤12 nm in size) remained in the metallic state, whereas NPs ≥ 15 nm became partially oxidized, suggesting that the latter were more readily able to dissociate CO. In contrast, in the presence of syngas, the oxide content of NPs ≥ 15 nm reduced, while it increased in quantity in the smaller NPs; this reoxidation that occurs primarily at the surface proved to be temporary, reforming the reduced state during subsequent UHV annealing. O K-edge measurements revealed that a key parameter mitigating the redox behaviour of the CoNPs were proximate oxygen vacancies (O_{vac}). These results demonstrate the differences in the reducibility and the reactivity of Co NP size on a Co/TiO₂ catalyst and the effect O_{vac} have on these properties, therefore yielding a better understanding of the physicochemical properties of this popular choice of FTS catalysts.



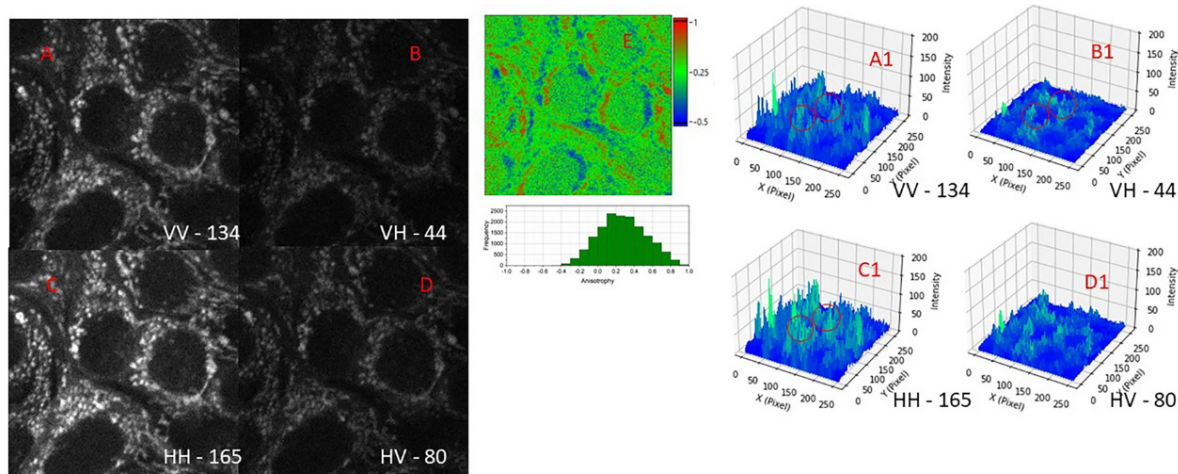
Reproduced from ACS Catal. 2023, 13, 15956-15966, under the terms of the CC-BY-4.0 license. doi: 10.1021/acscatal.3c03214

Authors: C. Qiu, Y. Odarchenko, Q. Meng, H. Dong, I. Lezcano Gonzalez, M. Panchal, P. Olalde-Velasco, F. Maccherozzi, L. Zanetti-Domingues, M.L. Martin-Fernandez, A.M. Beale ✉

The use of NADH anisotropy to investigate mitochondrial cristae alignment

Life may be expressed as the flow of electrons, protons, and other ions, resulting in large potential difference. It is also highly photo-sensitive, as a large proportion of the redox capable molecules it relies on are chromophoric. It is thus suggestive that a key organelle in eukaryotes, the mitochondrion, constantly adapt their morphology as part of the homeostatic process. Studying unstained in vivo nano-scale structure in live cells is technically very challenging.

One option is to study a central electron carrier in metabolism, reduced nicotinamide adenine dinucleotide (NADH), which is fluorescent and mostly located within mitochondria. The studies we describe present a novel avenue for exploring a possible fixed and ordered nature of NADH molecule particularly in mitochondria towards the beginning of understanding the other properties of the mitochondria, as well as the potential involvement of NADH in quantum biology.



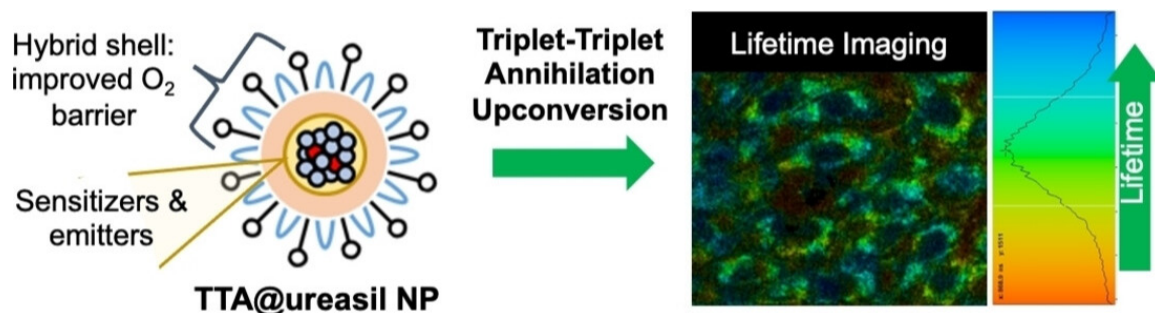
Two-photon fluorescence images of natural NADH in mitochondria from MCF7 cells. Time resolved decay profiles confirm NADH. Representative images from three repeat experiments. (A) is vertical excitation and vertical emission, (B) is vertical excitation, horizontal emission, (C) is horizontal excitation, vertical emission, (D) is horizontal excitation and horizontal emission. A1–D1 are the equivalent count profile plots where difference in intensities are reflected. Red circles also represent polarisation specific emissions, (E) is an anisotropy map of and pixel distributions. FoV 50 μm .

Taken from H.E. Smith, A.M. Mackenzie, C. Seddon, et al. The use of NADH anisotropy to investigate mitochondrial cristae alignment. Sci Rep 14, 5980 (2024) under the **CC-BY-4.0 license**. doi: 10.1038/s41598-024-55780-5

Authors: H.E. Smith, A.M. Mackenzie, C. Seddon, R. Mould, I. Kalampouka, P. Malakar, S.R. Needham, K. Beis, J.D. Bell, A. Nunn, **S.W. Botchway** ✉

Ultra-small air-stable triplet-triplet annihilation upconversion nanoparticles for anti-Stokes time-resolved imaging

Image contrast is often limited by background autofluorescence in steady-state bioimaging microscopy. Upconversion bioimaging can overcome this by shifting the emission lifetime and wavelength beyond the autofluorescence window. Here we demonstrate the first example of triplet-triplet annihilation upconversion (TTA-UC) based lifetime imaging microscopy. A new class of ultra-small nanoparticle (NP) probes based on TTA-UC chromophores encapsulated in an organic–inorganic host has been synthesised. The NPs exhibit bright UC emission (400–500 nm) in aerated aqueous media with a UC lifetime of $\approx 1\ \mu\text{s}$, excellent colloidal stability and little cytotoxicity. Proof-of-concept demonstration of TTA-UC lifetime imaging using these NPs shows that the long-lived anti-Stokes emission is easily discriminable from typical autofluorescence. Moreover, fluctuations in the UC lifetime can be used to map local oxygen diffusion across the subcellular structure. Our TTA-UC NPs are highly promising stains for lifetime imaging microscopy, affording excellent image contrast and potential for oxygen mapping that is ripe for further exploitation.



A new class of ultra-small nanoparticle (NP) probes based on triplet-triplet annihilation upconversion (TTA-UC) chromophores in an organic–inorganic ureasil host have been prepared and used to stain living cells as a proof-of-concept demonstration of TTA-UC lifetime imaging for the first time. Fluctuations of the UC lifetime in the stained cells indicate the NPs can be used to map local oxygen diffusion across the subcellular structure.

Reproduced from Angew. Chem. Int. Ed. 2023, 62, e202308602, under the terms of the **CC-BY-4.0 license**. doi:10.1002/anie.202308602

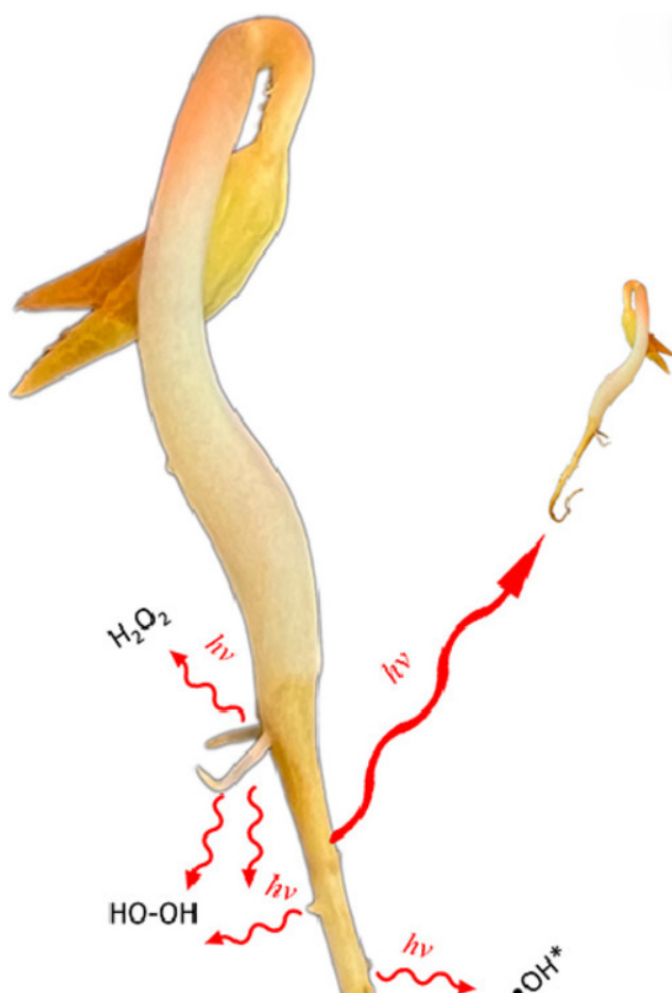
Authors: B. Zhang, K.D. Richards, B.E. Jones, A.R. Collins, R. Sanders, S.R. Needham, P. Qian, A. Mahadevegowda, C. Ducati, S.W. Botchway, **R.C. Evans** ✉

Rooting out ultraweak photon emission a-mung bean sprouts

It is well known that life has evolved to use and generate light, for instance, photosynthesis, vision and bioluminescence. What is less well known is that during normal metabolism, it can generate $1\text{--}100\text{ photons s}^{-1}\text{ cm}^{-2}$ known as ultra-weak photon emission (UPE), biophoton emission or biological autoluminescence.

We have established a highly sensitive experimental setup using opposing single photon detectors to study spontaneous and induced UPE in germinating mung beans, at stages from beans to leafy plants. Using this method, we observed a steady state photonic emission directly related to plant size, a temporary increase in emission in relation to dehydration and then rehydration, and an increase in photonic emission related to secondary root growth, possibly caused by increased cell division.

Our data therefore adds to the investigation of UPE which originates from the studies of the mitogenic effect first observed almost exactly a hundred years ago by Alexander Gurwitsch.

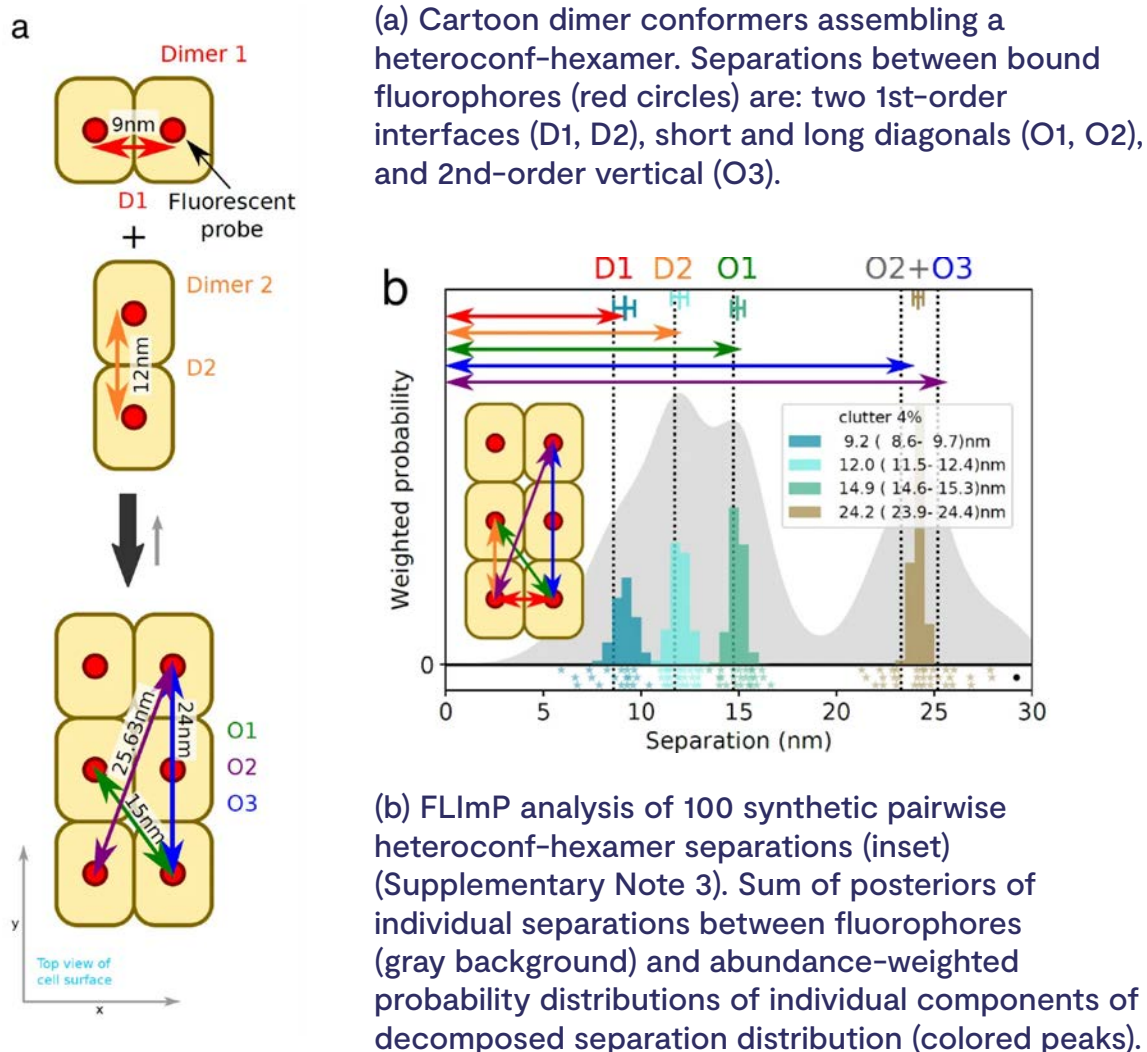


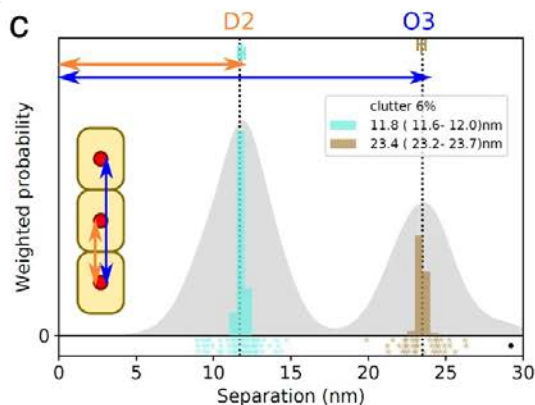
Taken from A.M. Mackenzie et al. Journal of Photochemistry and Photobiology 19 (2024) 100224 under the terms of the **CC-BY-4.0 license**. doi: 10.1016/j.jpap.2023.100224

Authors: A.M. Mackenzie ✉, H.E. Smith, R.R. Mould, J.D. Bell, A.V. Nunn, S.W. Botchway ✉

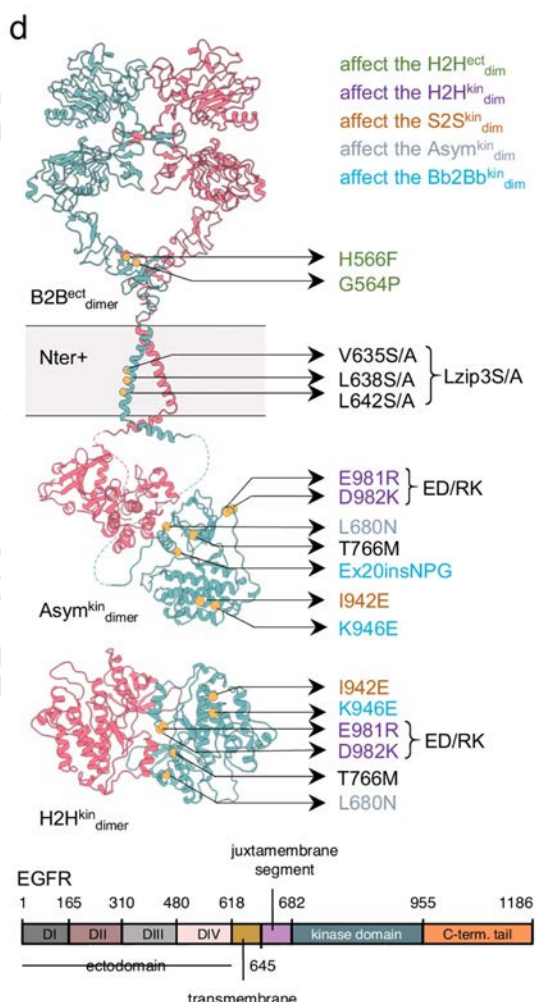
Drug-resistant EGFR mutations promote lung cancer by stabilizing interfaces in ligand-free kinase-active EGFR oligomers

The Epidermal Growth Factor Receptor (EGFR) is frequently found to be mutated in non-small cell lung cancer. Oncogenic EGFR has been successfully targeted by tyrosine kinase inhibitors, but acquired drug resistance eventually overcomes the efficacy of these treatments. Attempts to surmount this therapeutic challenge are hindered by a poor understanding of how and why cancer mutations specifically amplify ligand-independent EGFR auto-phosphorylation signals to enhance cell survival and how this amplification is related to ligand-dependent cell proliferation. Here we show that drug-resistant EGFR mutations manipulate the assembly of ligand-free, kinase-active oligomers to promote and stabilize the assembly of oligomer-obligate active dimer sub-units and circumvent the need for ligand binding. We reveal the structure and assembly mechanisms of these ligand-free, kinase-active oligomers, uncovering oncogenic functions for hitherto orphan transmembrane and kinase interfaces, and for the ectodomain tethered conformation of EGFR. Importantly, we find that the active dimer sub-units within ligand-free oligomers are the high affinity binding sites competent to bind physiological ligand concentrations and thus drive tumour growth, revealing a link with tumour proliferation. Our findings provide a framework for future drug discovery directed at tackling oncogenic EGFR mutations by disabling oligomer-assembling interactions.

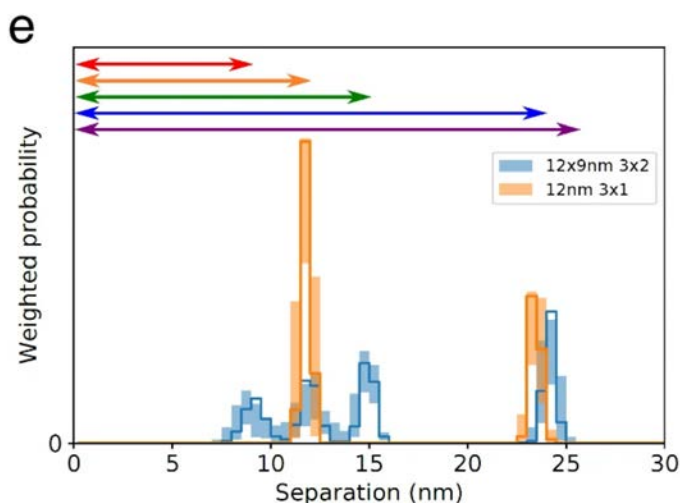




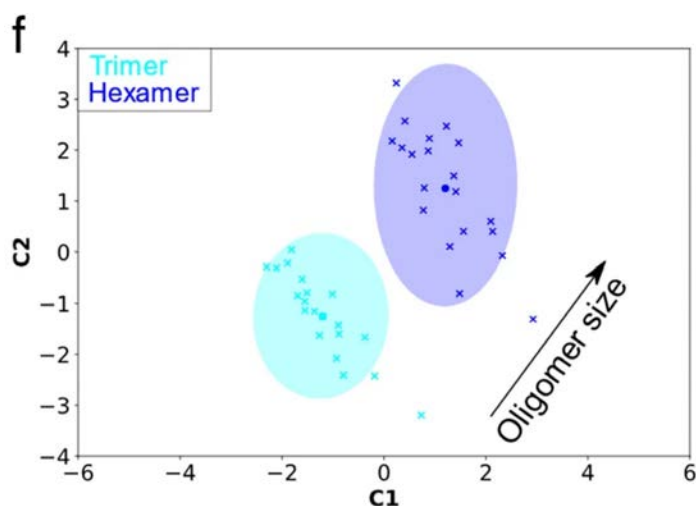
(c) As (b) for the homo-trimer formed by the Dimer 2 conformer.



(d) Top, map of mutations and treatments superimposed on the B2BectdimerCR8181, an Asymkindimer3, and H2Hkindimer54 sub-units. Mutations colored according to the different dimer conformers they inhibit or disrupt. Bottom, EGFR sequence diagram.



(e) Comparisons between decomposed separation probability distributions between datasets.



(f) Wasserstein MDS analysis of FLImP decompositions. This measures the work needed to convert a decomposed separation set into another, thereby estimating similarities and differences between whole FLImP separation decompositions.

Reproduced from R.S. Iyer, S.R. Needham, I. Galdadas et al. Drug-resistant EGFR mutations promote lung cancer by stabilizing interfaces in ligand-free kinase-active EGFR oligomers. Nat Commun 15, 2130 (2024) under the terms of the **CC-BY-4.0 license**. doi: 10.1038/s41467-024-46284-x

Authors: R.S. Iyer, S.R. Needham, I. Gladadas, B.M. Davis, S.K. Roberts, R.C.H. Man, L.C. Zanetti-Domingues, D.T. Clarke, G.O. Fruhwirth, P.J. Parker, **D.J. Rolfe** ✉, **F.L. Gervasio** ✉, **M.L. Martin-Fernandez** ✉

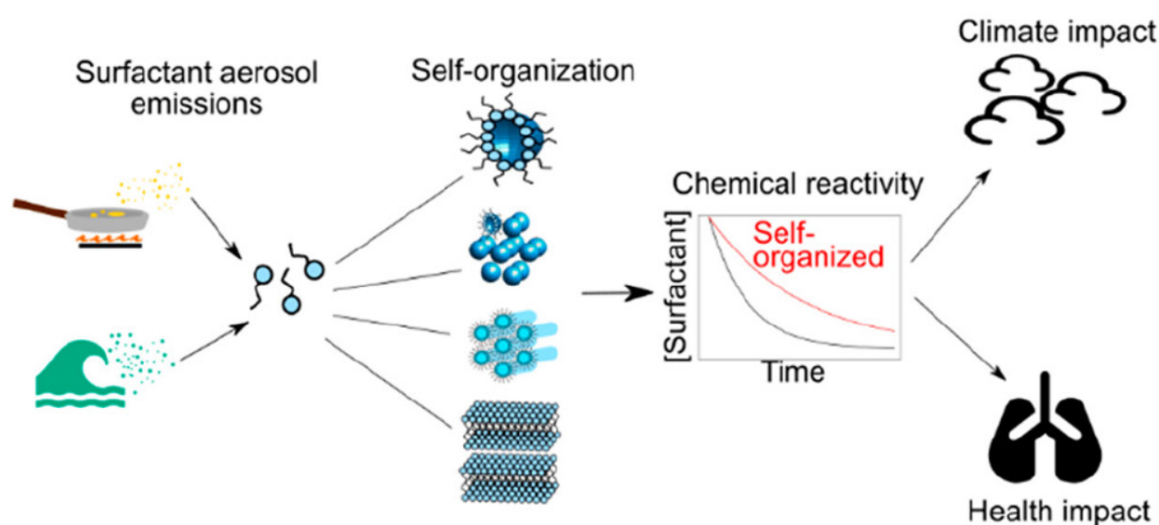
Molecular self-organization in surfactant atmospheric aerosol proxies

Aerosols are ubiquitous in the atmosphere, both outdoors and indoors. Surfactants make significant contributions to aerosol emissions, with sources ranging from cooking to sea spray. These molecules alter the cloud droplet formation potential by changing the surface tension of aqueous droplets and thus increasing their ability to grow. They can also coat solid surfaces such as windows (“window grime”) and dust particles.

A common cooking and marine emission, oleic acid, is known to self-organise into a range of 3-D nanostructures, which are highly viscous and as such can impact the kinetics of aerosol and film ageing.

Most literature studies on oleic acid oxidation have focused on pure liquid oleic acid in its native form either as particles, deposited films, or monolayers, occasionally mixed with cosurfactants. Our work represents a new avenue, focusing on how the surfactant itself is organised and how this self-organisation could impact the key aerosol processes of water uptake and chemical reaction outdoors and indoors.

We created a body of experimental and modelling work to study self-organised proxies as nanometre-to-micrometre films, levitated droplets, and bulk mixtures. Our findings suggest that hazardous, reactive materials may be protected in aerosol matrices underneath a highly viscous shell, thus extending the atmospheric residence times of otherwise short-lived species.

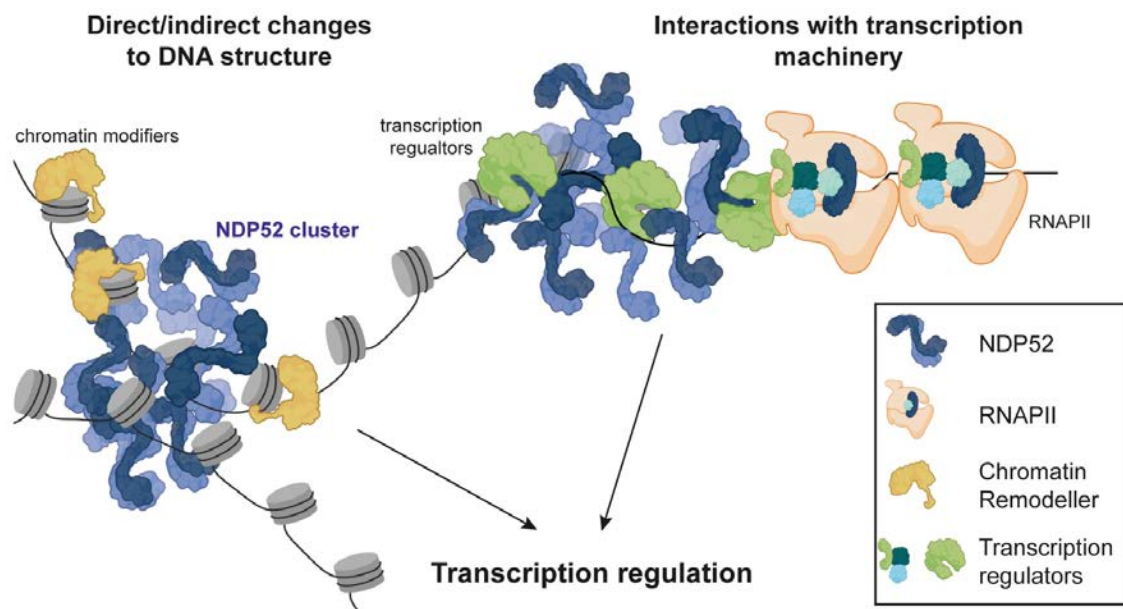


Taken from Acc. Chem. Res. 2023, 56, 19, 2555–2568 published by the American Chemical Society under the terms of the **CC-BY-4.0 license**. doi: 10.1021/acs.accounts.3c00194

Authors: A. Milsom, A.M. Squires, A.D. Ward, C. Pfrang ✉

Autophagy receptor NDP52 alters DNA conformation to modulate RNA polymerase II transcription

NDP52 is an autophagy receptor involved in the recognition and degradation of invading pathogens and damaged organelles. Although NDP52 was first identified in the nucleus and is expressed throughout the cell, to date, there is no clear nuclear functions for NDP52. Here, we use a multidisciplinary approach to characterise the biochemical properties and nuclear roles of NDP52. We find that NDP52 clusters with RNA Polymerase II (RNAPII) at transcription initiation sites and that its overexpression promotes the formation of additional transcriptional clusters. We also show that depletion of NDP52 impacts overall gene expression levels in two model mammalian cells, and that transcription inhibition affects the spatial organisation and molecular dynamics of NDP52 in the nucleus. This directly links NDP52 to a role in RNAPII-dependent transcription. Furthermore, we also show that NDP52 binds specifically and with high affinity to double-stranded DNA (dsDNA) and that this interaction leads to changes in DNA structure in vitro. This, together with our proteomics data indicating enrichment for interactions with nucleosome remodelling proteins and DNA structure regulators, suggests a possible function for NDP52 in chromatin regulation. Overall, here we uncover nuclear roles for NDP52 in gene expression and DNA structure regulation.



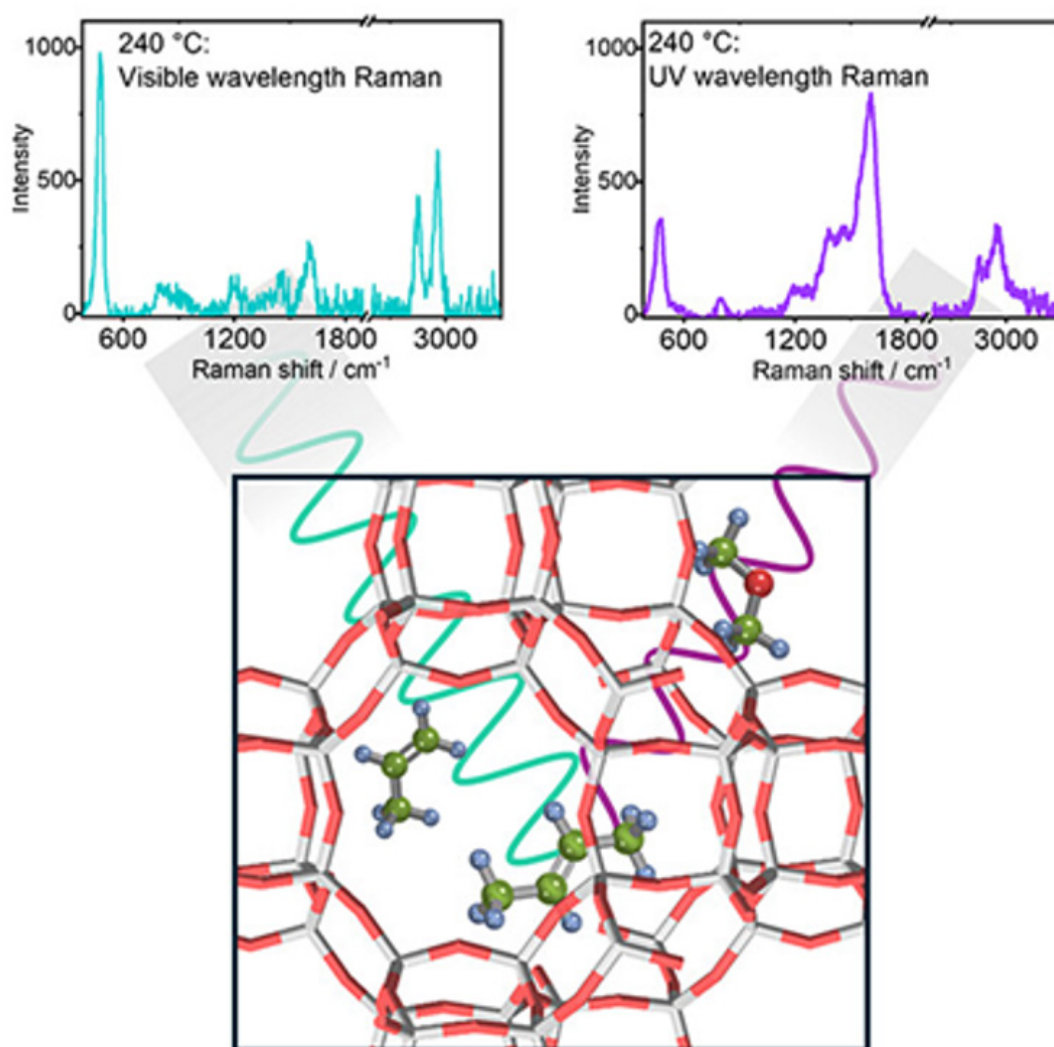
Model of possible mechanism for NDP52's activity in transcription. NDP52 could directly interact with DNA in the nucleus, or with chromatin modifiers (e.g. histone modifiers), to cause local changes to chromatin structure. Conversely, interactions with transcription factors/coactivators and transcription machinery could also modulate transcription activity of genes. Created with BioRender.com.

Reproduced from dos Á Santos, D.E. Rollins, Y. Hari-Gupta, et al. Autophagy receptor NDP52 alters DNA conformation to modulate RNA polymerase II transcription. Nat Commun 14, 2855 (2023) under the terms of the **CC-BY-4.0 license**. doi: 10.1038/s41467-023-38572-9

Authors: Á. dos Santos, D.E. Rollins, Y. Hari-Gupta, H. McArthur, M. Du, S. Yong Zi Ru, K. Pidlisna, A. Stranger, F. Lorgat, D. Lambert, I. Brown, K. Howland, J. Aaron, L. Wang, P.J.I. Ellis, T.-L. Chew, M. Martin-Fernandez, A.L.B. Pyne, **C.P. Toseland** ✉

Methanol-to-olefins studied by UV Raman spectroscopy as compared to visible wavelength: Capitalization on resonance enhancement

Resonance Raman spectroscopy can provide insights into complex reaction mechanisms by selectively enhancing the signals of specific molecular species. In this work, we demonstrate that, by changing the excitation wavelength, Raman bands of different intermediates in the methanol-to-hydrocarbons reactions can be identified. We show in particular how UV excitation enhances signals from short-chain olefins and cyclopentadienyl cations during the induction period, while visible excitation better detects later-stage aromatics. However, visible excitation is prone to fluorescence that can obscure Raman signals, and hence, we show how fast fluorescence rejection techniques like Kerr gating are necessary for extracting useful information from visible excitation measurements.

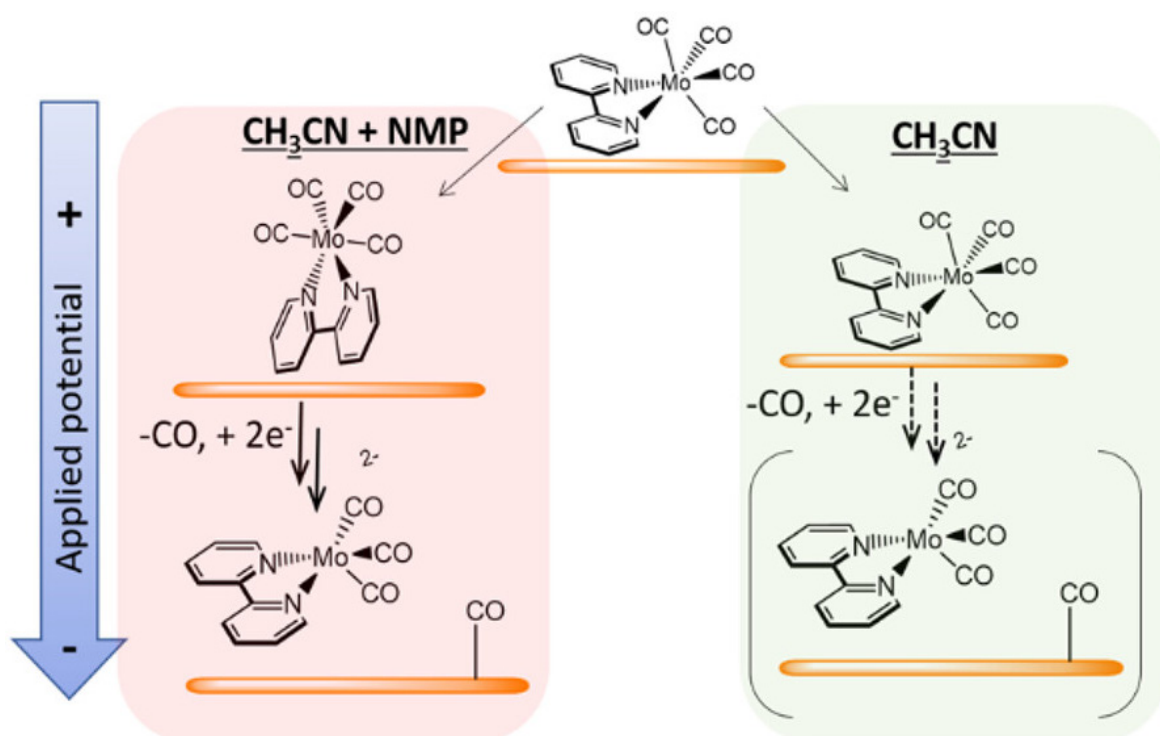


Reproduced from J. Phys. Chem. Lett. 2024, 15, 26, 6826–6834, published by the American Chemical Society under the terms of the **CC-BY-4.0 license**. doi: 10.1021/acs.jpcllett.4c00865

Authors: E. Campbell, I.V. Sazanovich, M. Towrie, M.J. Watson, I. Lezcano-Gonzalez ✉, A.M. Beale ✉

Potential dependent reorientation controlling activity of a molecular electrocatalyst

The activity of molecular electrocatalysts depends on the interplay of electrolyte composition near the electrode surface, the composition and morphology of the electrode surface, and the electric field at the electrode–electrolyte interface. This interplay is challenging to study and often overlooked when assessing molecular catalyst activity. Here, we use surface specific vibrational sum frequency generation (VSFG) spectroscopy to study the solvent and potential dependent activation of $\text{Mo}(\text{bpy})(\text{CO})_4$, a CO_2 reduction catalyst, at a polycrystalline Au electrode. We find that the parent complex undergoes potential dependent reorientation at the electrode surface when a small amount of *N*-methyl-2-pyrrolidone (NMP) is present. This preactivates the complex, resulting in greater yields at less negative potentials, of the active electrocatalyst for CO_2 reduction.



The large increase in electrocatalytic activity of $\text{Mo}(\text{bpy})(\text{CO})_4$ when a small (10% vol.) amount of NMP is added to an electrolyte solution is shown to be due to a potential dependent solvent restructuring of the double layer that leads to reorientation of $\text{Mo}(\text{bpy})(\text{CO})_4$ at the electrode surface.

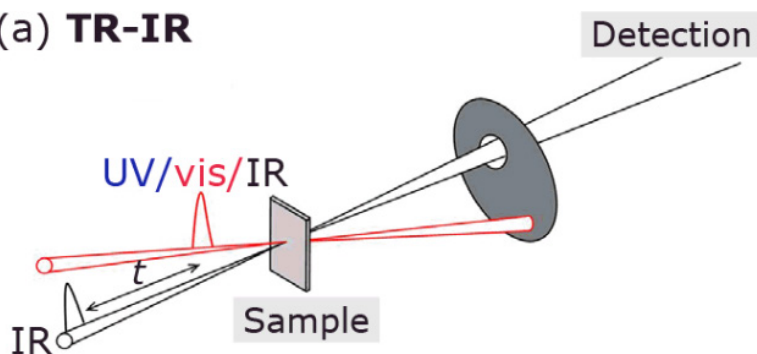
Reproduced from J. Am. Chem. Soc. 2024, 146, 11, 7130–7134 published by American Chemical Society under the terms of the **CC-BY-4.0 license**. doi: 10.1021/jacs.3c13076

Authors: A.M. Gardner, G. Neri, B. Siritanaratkul, H. Jang, K.H. Saeed, P.M. Donaldson, **A.J. Cowan** ✉

Ultrafast spectroscopy at the Central Laser Facility: Applications to the study of commercially relevant materials

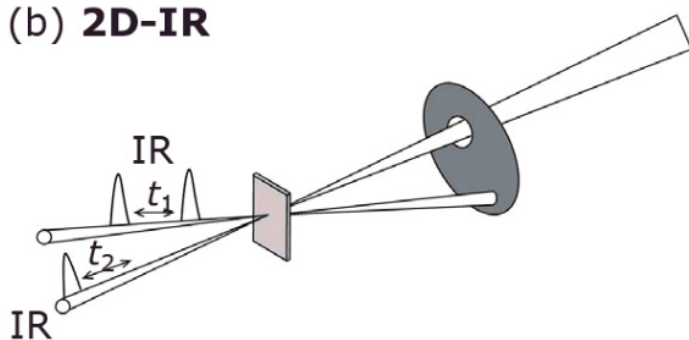
In this article, we will examine ultrafast spectroscopy techniques and applications, covering time-resolved infrared (TR-IR) spectroscopy, time resolved visible (TA) spectroscopy, two-dimensional infrared (2D-IR) spectroscopy, Kerr-gated Raman spectroscopy, time-resolved Raman and surface sum-frequency generation (SSFG) spectroscopy. In addition to introducing each technique, we will cover some basics, such as what kinds of lasers are used and discuss how these techniques are applied to study a diversity of chemical problems such as photocatalysis, photochemistry, electrocatalysis, battery electrode characterisation, zeolite characterisation and protein structural dynamics.

(a) TR-IR



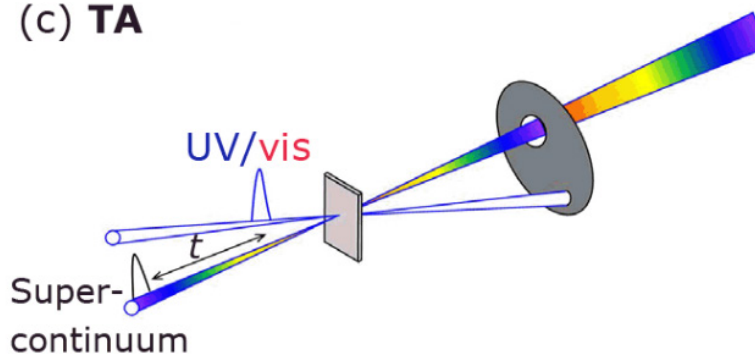
Example laser beam configurations for ultrafast spectroscopy: (a) TR-IR with UV-visible-IR pumping

(b) 2D-IR



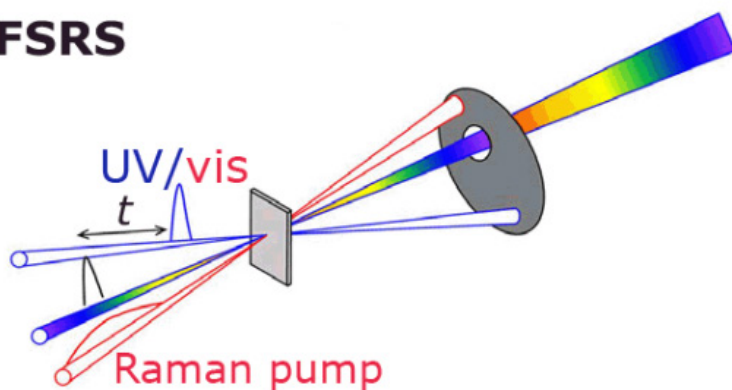
(b) 2D-IR

(c) TA



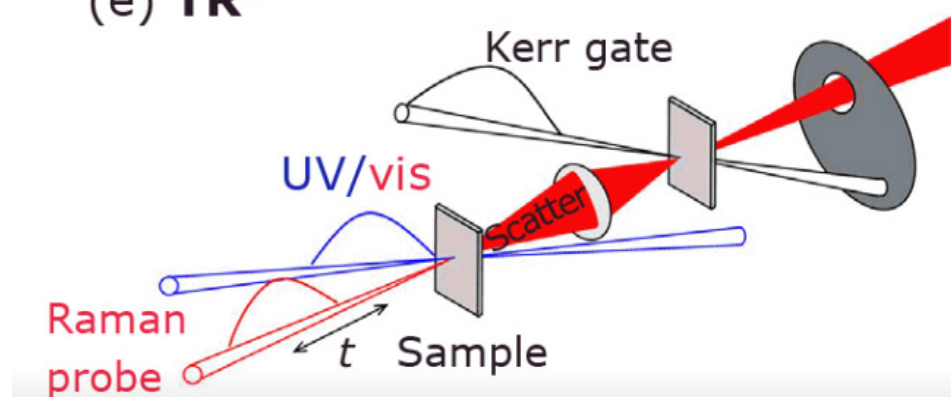
(c) TA (transient visible absorption spectroscopy)

(d) **FSRS**



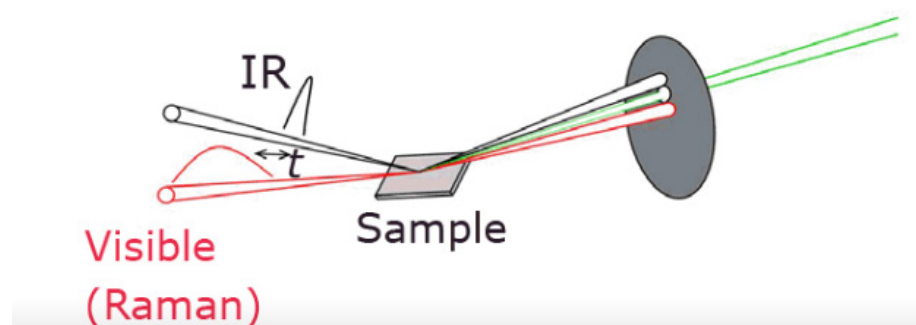
(d) FSRS

(e) **TR³**



(e) Kerr-gated TR3

(f) **IR-vis SSFG**



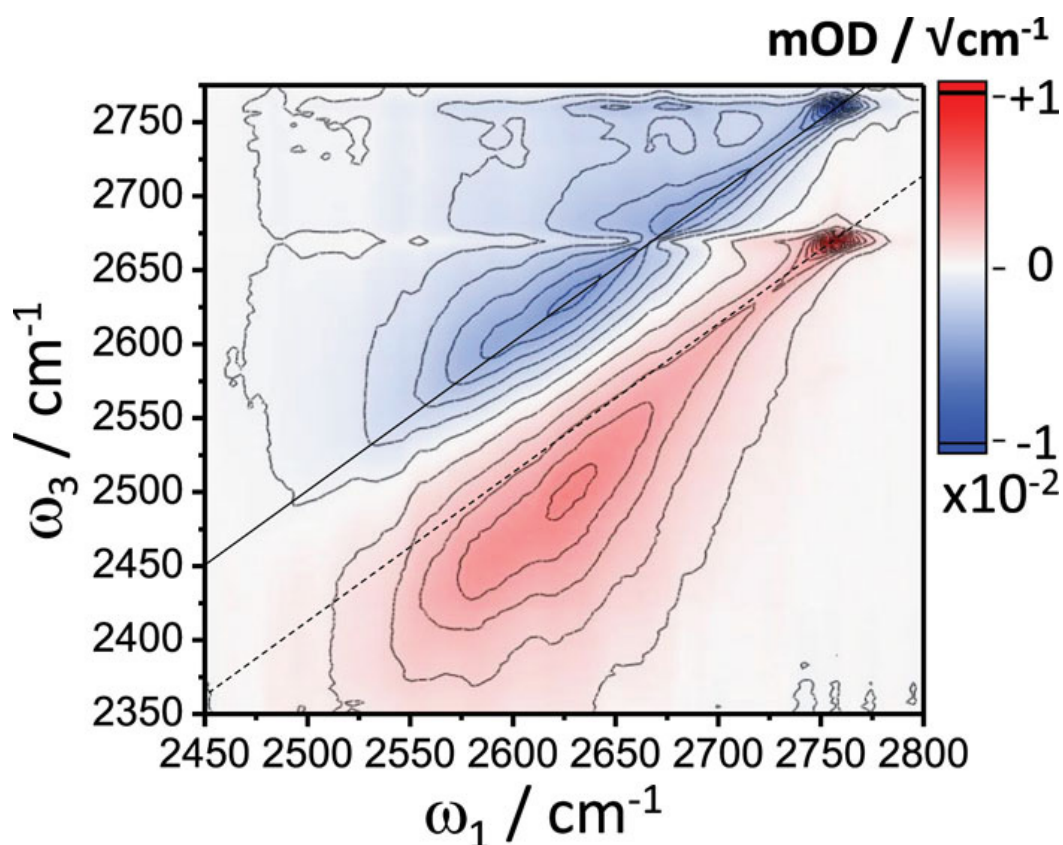
(f) IR-visible SSFG

Reproduced from Johnson Matthey Technol. Rev., 2024, 68, (4), 503–520, published by Johnson Matthey under the terms of the **CC-BY-4.0 license**. doi: 10.1595/205651324X17092043851525

Authors: P.M. Donaldson ✉, I.V. Sazanovich, P. Malakar, S. Maiti, M. Towrie, G.M. Greetham ✉

The 2D-IR spectrum of hydrogen-bonded silanol groups in pyrogenic silica

Pyrogenic silica is a form of amorphous silica with a high surface area and a heterogeneous distribution of silanol hydroxyl terminations and defects. In this work, the interesting and unusual form of the hydroxyl-stretch 2D-IR spectrum of pyrogenic silica is presented and explored in the deuterated (deuteroxyl) form. Transition dipole couplings between hydrogen-bonded and non-hydrogen-bonded silanol groups give a distinct cross-peak in the 2D-IR spectrum, displaying interstate coherence oscillations during the 2D-IR experimental waiting time. The strong asymmetry about the diagonal is proposed to be the result of both the relatively small transition dipole coupling strength and the extreme differences in the width of the hydrogen-bonded and non-hydrogen-bonded silanol bands. The resulting interference of negative and positive cross-peaks has minimal intensity in the below-diagonal $\omega_3 < \omega_1$ region of the spectrum. An additional strong positive cross-peak is observed at a position in the 2D-IR spectrum inconsistent with transition dipole coupling. An assignment as a fifth order effect is proposed.



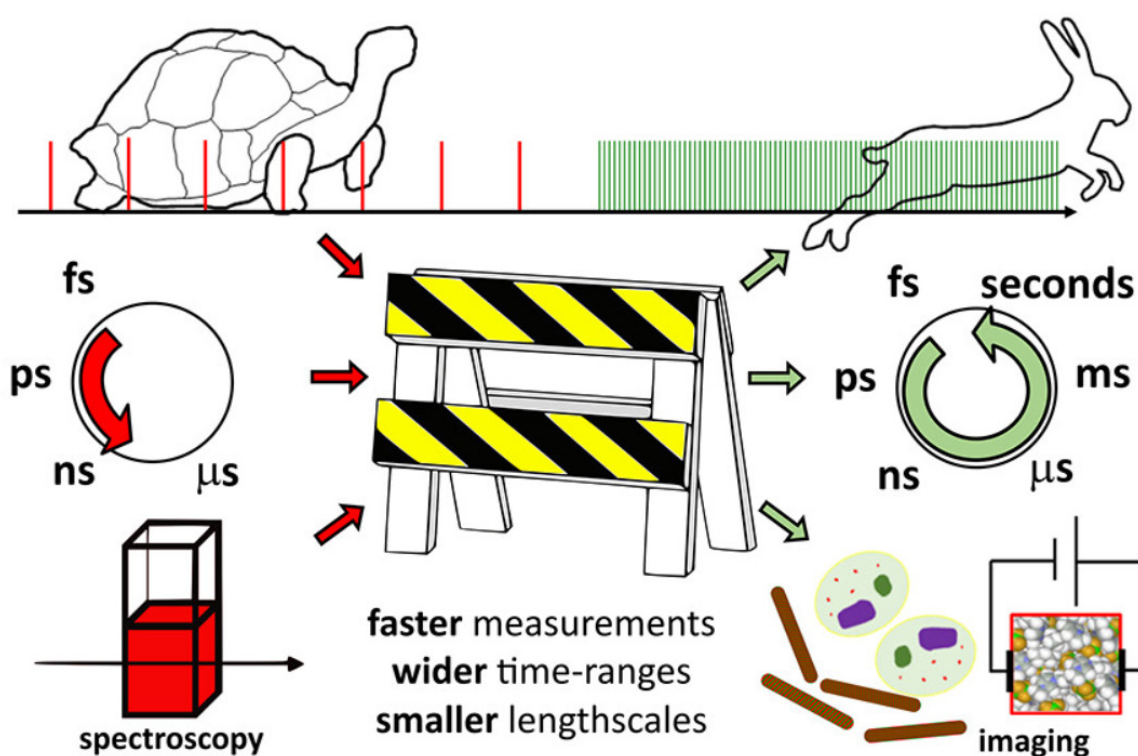
The 2D-IR spectrum of deuterated pyrogenic silica held at 175 °C. The diagonal of the spectrum is indicated by a solid black line. The dotted line parallel to the diagonal is offset by the non-hydrogen-bonded SiOD anharmonicity Δ_b , revealing the increase in anharmonicity with decreasing wavenumber. The waiting time (t_2) is 600 fs and polarization $\langle \text{XXYY} \rangle$. The first five contour lines reach an amplitude of $5 \times 10^{-3} \text{ mOD}/\sqrt{\text{cm}^{-1}}$.

Reproduced from J. Chem. Phys. 160, 104204 (2024) under the **CC-BY-4.0** license.
doi: 10.1063/5.0193551

Author: P.M. Donaldson ✉

Breaking barriers in ultrafast spectroscopy and imaging using 100 kHz amplified Yb-laser systems

There is now a technology shift occurring in ultrafast spectroscopy, made possible by new Yb-based lasers, that is opening exciting new experiments in the chemical and physical sciences. Amplified Yb-based lasers are not only more compact and efficient than their predecessors but also, most importantly, operate at many times the repetition rate with improved noise characteristics in comparison to the previous generation of Ti:sapphire amplifier technologies. Taken together, these attributes are enabling new experiments, generating improvements to long-standing techniques, and affording the transformation of spectroscopies to microscopies. This Account aims to show that the shift to 100 kHz lasers is a transformative step in nonlinear spectroscopy and imaging. We are convinced that Yb-based 100 kHz laser systems will soon become a standard of femtosecond laser technology, replacing many Ti:Sapphire lasers applications. Their improved parameters will not only make already existing experiments easier, better, and faster, but also allow for conceptually new experiments and lower barriers to starting an ultrafast spectroscopy laboratory.

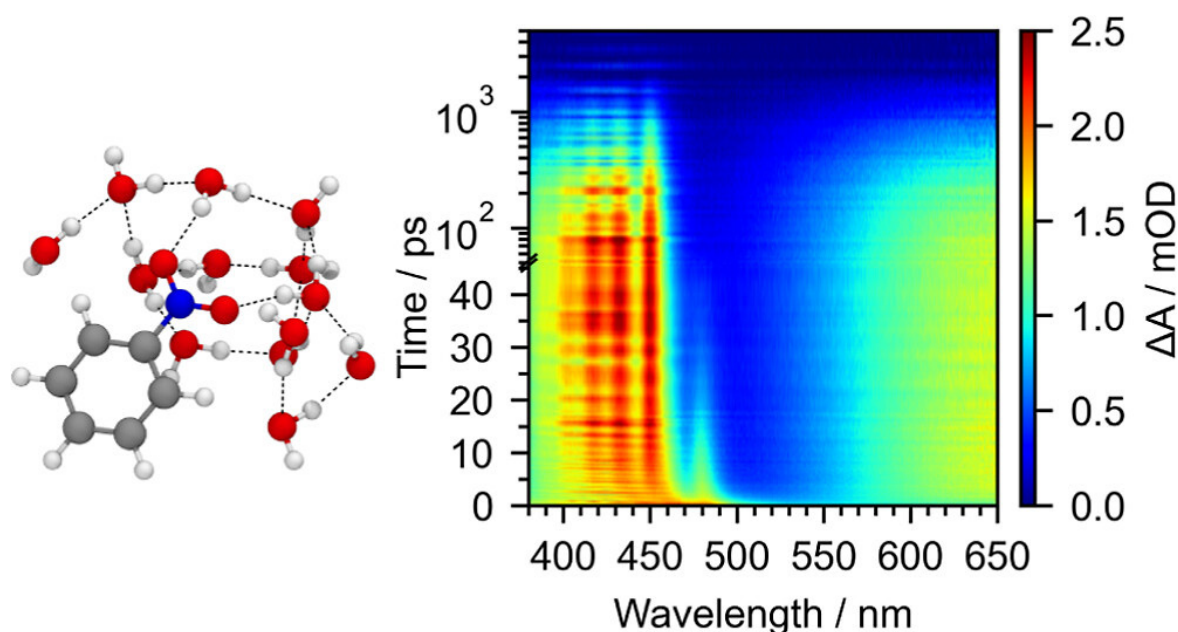


Taken from Acc. Chem. Res. 2023, 56, 15, 2062–2071, published by American Chemical Society under the terms of the **CC-BY-4.0 license**. doi: 10.1021/acs.accounts.3c00152

Authors: P.M. Donaldson ✉, G.M. Greetham, C.T. Middleton, B.M. Luther, M.T. Zanni, P. Hamm ✉, A.T. Krummel ✉

Unravelling the ultrafast photochemical dynamics of nitrobenzene in aqueous solution

Nitroaromatic compounds are major constituents of the brown carbon aerosol particles in the troposphere that absorb near-ultraviolet (UV) and visible solar radiation and have a profound effect on the Earth's climate. The primary sources of brown carbon include biomass burning, forest fires, and residential burning of biofuels, and an important secondary source is photochemistry in aqueous cloud and fog droplets. Nitrobenzene is the smallest nitroaromatic molecule and a model for the photochemical behavior of larger nitroaromatic compounds. Despite the obvious importance of its droplet photochemistry to the atmospheric environment, there have not been any detailed studies of the ultrafast photochemical dynamics of nitrobenzene in aqueous solution. Here, we combine femtosecond transient absorption spectroscopy, time-resolved infrared spectroscopy, and quantum chemistry calculations to investigate the primary steps following the near-UV ($\lambda \geq 340$ nm) photoexcitation of aqueous nitrobenzene. To understand the role of the surrounding water molecules in the photochemical dynamics of nitrobenzene, we compare the results of these investigations with analogous measurements in solutions of methanol, acetonitrile, and cyclohexane. We find that vibrational energy transfer to the aqueous environment quenches internal excitation, and therefore, unlike the gas phase, we do not observe any evidence for formation of photoproducts on timescales up to 500 ns. We also find that hydrogen bonding between nitrobenzene and surrounding water molecules slows the S_1/S_0 internal conversion process.



On the left: the calculated microsolvated structure of nitrobenzene in water environment. On the right: 2D-plot representation of the Transient Absorption data for nitrobenzene in water.

Reproduced from J. Am. Chem. Soc. 2024, 146, 15, 10407–10417, published by American Chemical Society under the terms of the **CC-BY-4.0 license**. doi: 10.1021/jacs.3c13826

Authors: N.A. Lau, D. Ghosh, S. Bourne-Worster, R. Kumar, W.A. Whitaker, J. Heitland, J.A. Davies, G. Karras, I.P. Clark, G.M. Greetham, G.A. Worth, A.J. Orr-Ewing, **H.H. Fielding** ✉

Background correction of time-resolved infrared spectroscopy data for the ‘tricky’ transcriptional regulator protein, B₁₂-dependent CarH

Time-resolved infrared (TRIR) spectroscopy is a powerful method providing information on excited state dynamics, conformational changes, intermolecular interactions and solvation. However, TRIR measurements on biological samples can be challenging, particularly when working close to the detection limit due to low sample concentration. This article will discuss how we correct for a delay-dependent step-like background pattern attributed to the detectors from the Central Laser Facilities LIFETIME instrument. TRIR data were collected for wildtype and variant chromophore binding domains of the photoreceptor protein B₁₂-dependent CarH, in addition to the full-length protein bound to DNA. This work may be of use to those who study challenging biological samples that are limited in quantity and/or produce low signals where background signal hinders a meaningful kinetic analysis. It also builds on our previous study, where we introduced a new method for handling/measuring light sensitive proteins in small volumes.

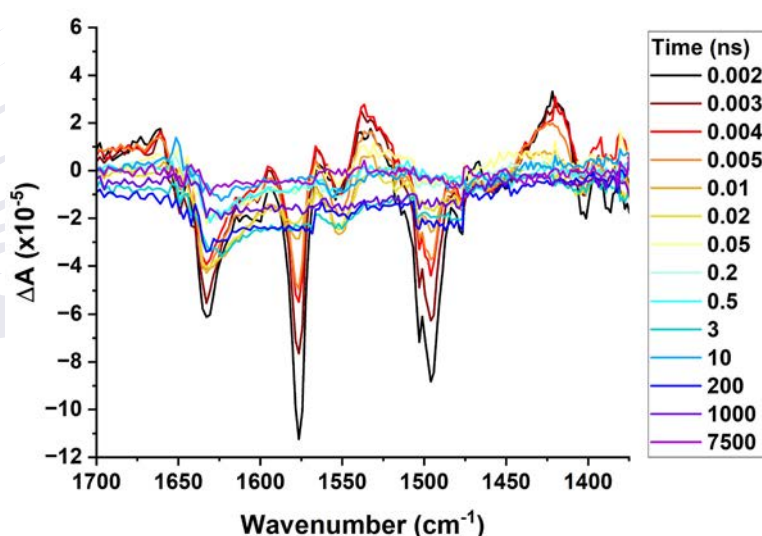


Figure 1: Raw TRIR difference spectra for T-WT CarH relative to the ground state between 2 ps–7.5 μ s following photoexcitation at 525 nm and averaged over five repeats. A block-like background pattern is evident, which originates from the detector and varies with delay time.

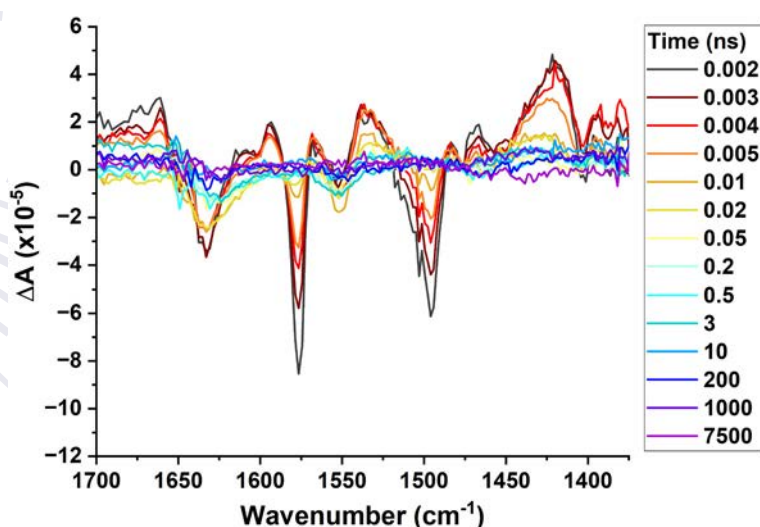
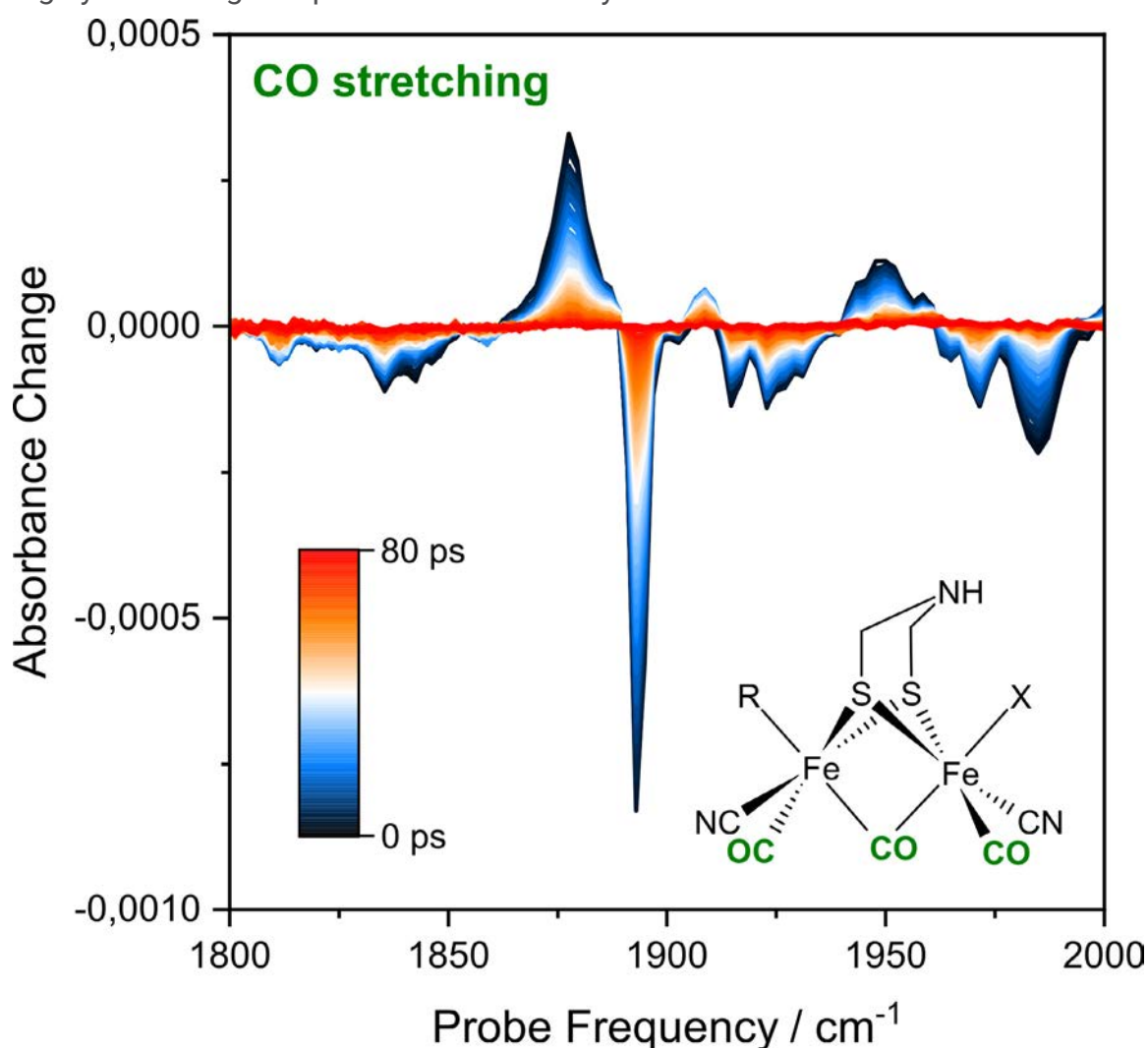


Figure 2: Corrected TRIR difference spectra for T-WT CarH relative to the ground state between 2 ps–7.5 μ s following photoexcitation at 525 nm and averaged over five repeats. The block-like background pattern evident in the raw data has been removed.


Authors: E. Wall, I.V. Sazanovich, M. Kurttila, I.S. Camacho, N.T. Hunt, A.R. Jones, S. Hay ✉

Progress in the 2D-IR characterisation of hydrogenases at Ultra

Hydrogenases are metalloenzymes that catalyse the cleavage and evolution of molecular hydrogen (H_2), a perfectly clean fuel. Due to the presence of biologically uncommon CO and CN⁻ ligands at the catalytic metal sites of hydrogenases, infrared (IR) spectroscopy is an ideal technique for studying these enzymes. 2D-IR and $IR_{\text{pump}}-IR_{\text{probe}}$ experiments performed at Ultra have previously gained detailed insights into the structure and dynamics of [NiFe] hydrogenases that cannot be obtained by linear IR absorption spectroscopy. Here we report on a twofold extension of this approach. On the one hand, we have obtained, for the first time, nonlinear IR spectra of more complex [FeFe] hydrogenases (see Figure). On the other hand, preliminary *in vivo* 2D-IR spectra of a [NiFe] hydrogenase within live cells were obtained by using an approach for probing highly scattering samples that was recently established at Ultra.

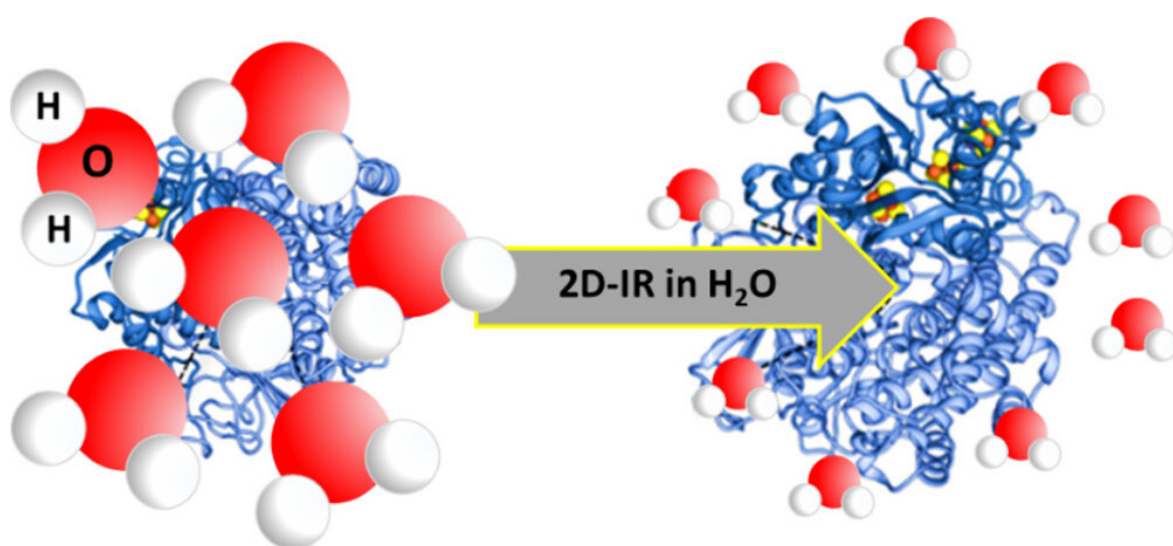


$IR_{\text{pump}}-IR_{\text{probe}}$ spectrum of reduced [FeFe] hydrogenase. Signals reflect stretching vibrations of CO ligands bound to the active site (see inset).

Authors: C.C.M. Bernitzky, M. Horch , D.M. Vaithyanathan, P. Donaldson, G.M. Greetham, I. Sazanovich, O. Lenz, J. Schoknecht, J.A. Birrell, P. Rodríguez Maciá

Using 2D-IR Spectroscopy to Measure the Structure, Dynamics, and Intermolecular Interactions of Proteins in H₂O

Infrared (IR) spectroscopy probes molecular structure at the level of the chemical bond or functional group. In this Account, a series of studies applying 2D-IR to study the spectroscopy and dynamics of proteins in H₂O-rich solvents is reviewed. A comparison of IR absorption spectroscopy and 2D-IR spectroscopy of protein-containing fluids is used to demonstrate the basis of the approach before a series of applications is presented. These range from measurements of fundamental protein biophysics to recent applications of machine learning to gain insight into protein–drug binding in complex mixtures. An outlook is presented, considering the potential for 2D-IR measurements to contribute to our understanding of protein behaviour under near-physiological conditions, along with an evaluation of the obstacles that still need to be overcome.



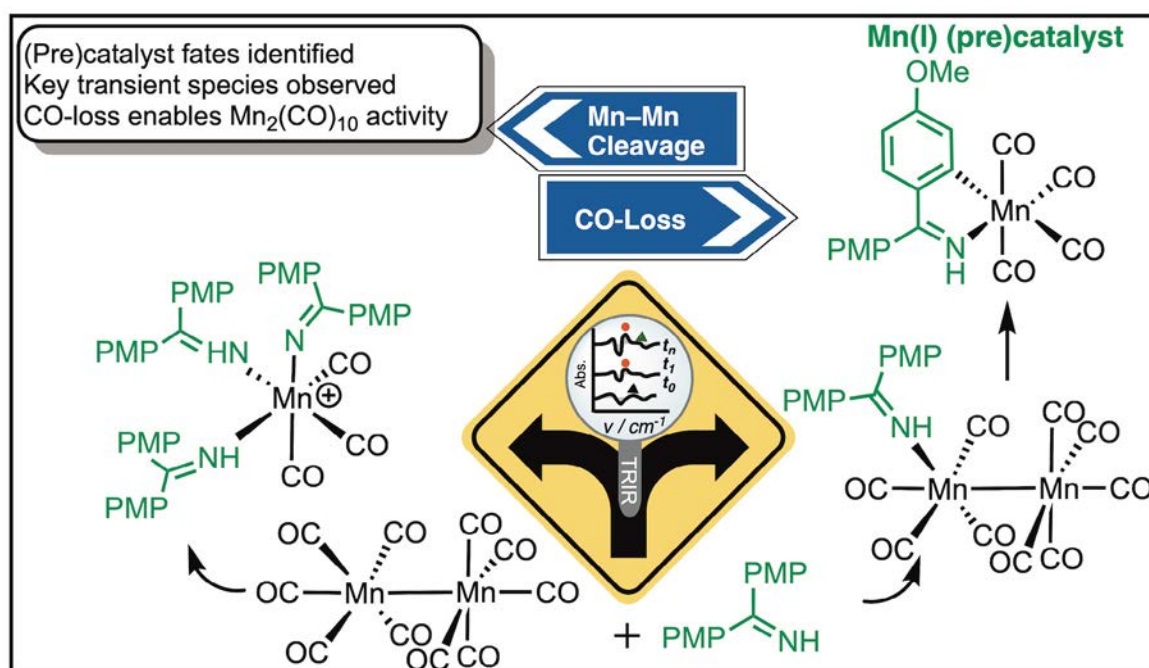
2D-IR spectroscopy can provide the ability to measure protein amide I spectra in H₂O-rich solutions without the need for isotopic substitution or complex data processing.

Taken from Acc. Chem. Res. 2024, 57, 5, 685–692 published by the American Chemical Society under the terms of the **CC-BY-4.0 license**. doi: 10.1021/acs.accounts.3c00682

Authors: N.T. Hunt ✉

The importance of understanding (pre)catalyst activation in versatile C–H bond functionalisations catalysed by $[\text{Mn}_2(\text{CO})_{10}]$

Mn-catalysed reactions offer great potential in synthetic organic and organometallic chemistry and the success of Mn carbonyl complexes as (pre) catalysts hinges on their stabilisation by strong field ligands enabling Mn(I)-based, redox neutral, catalytic cycles. The mechanistic processes underpinning the activation of the ubiquitous Mn(0) (pre)catalyst $[\text{Mn}_2(\text{CO})_{10}]$ in C–H bond functionalisation reactions is now reported for the first time. By combining time-resolved infra-red (TRIR) spectroscopy on a ps–ms timescale and *in operando* studies using *in situ* infra-red spectroscopy, insight into the microscopic bond activation processes which lead to the catalytic activity of $[\text{Mn}_2(\text{CO})_{10}]$ has been gained. Using an exemplar system, based on the annulation between an imine, 1, and Ph_2C_2 , 2, TRIR spectroscopy enabled the key intermediate $[\text{Mn}_2(\text{CO})_9(1)]$, formed by CO loss from $[\text{Mn}_2(\text{CO})_{10}]$, to be identified. *In operando* studies demonstrate that $[\text{Mn}_2(\text{CO})_9(1)]$ is also formed from $[\text{Mn}_2(\text{CO})_{10}]$ under the catalytic conditions and is converted into a mononuclear manganacycle, $[\text{Mn}(\text{CO})_4(\text{C}^*\text{N})]$ (C^*N = cyclometallated imine), a second molecule of 1 acts as the oxidant which is, in turn, reduced to an amine. As $[\text{Mn}(\text{CO})_4(\text{C}^*\text{N})]$ complexes are catalytically competent, a direct route from $[\text{Mn}_2(\text{CO})_{10}]$ into the Mn(I) catalytic reaction coordinate has been determined. Critically, the mechanistic differences between $[\text{Mn}_2(\text{CO})_{10}]$ and Mn(I) (pre)catalysts have been delineated, informing future catalyst screening studies.

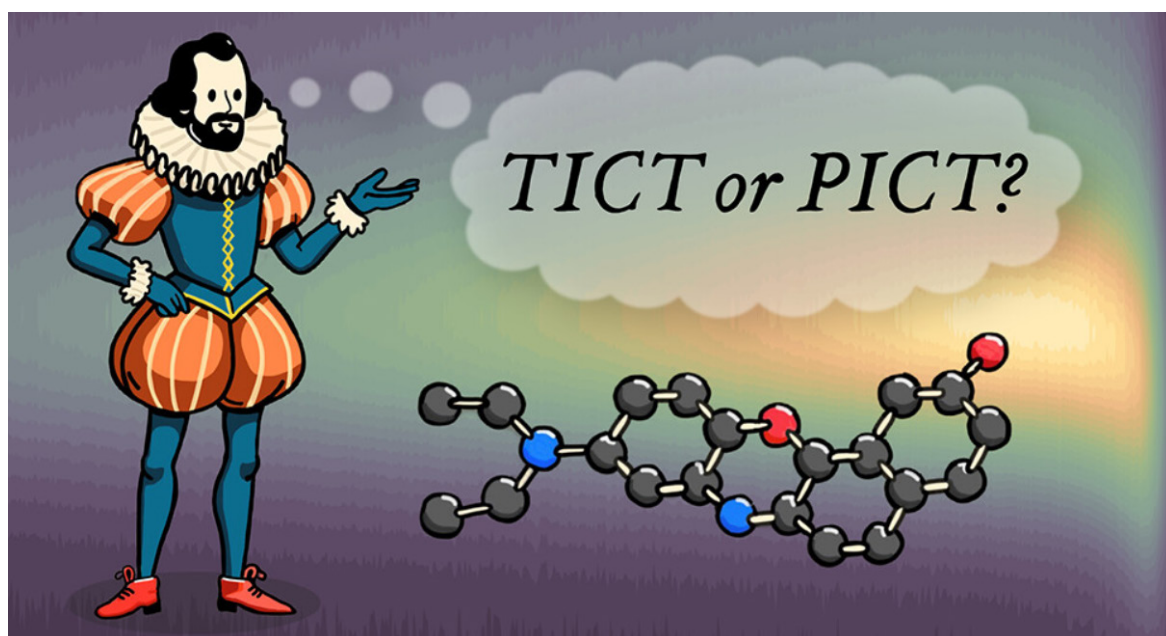


Reproduced from Chem. Sci., 2024, 15, 9183 published by the Royal Society of Chemistry under the terms of the **CC-BY-3.0 license**. doi: 10.1039/d4sc01215a

Authors: J.B. Eastwood, T.J. Burden, L. Anders Hammarback, C. Horbaczewski, T.F.N. Tanner, I.P. Clark, G.M. Greetham, M. Towrie, **I.J.S. Fairlamb** ✉, **J.M. Lynam** ✉

Nile Red fluorescence: Where's the twist?

Nile Red is a fluorescent dye used extensively in bioimaging due to its strong solvatochromism. The photophysics underpinning Nile Red's fluorescence has been disputed for decades, with some studies claiming that the dye fluoresces from two excited states and/or that the main emissive state is twisted and intramolecular charge-transfer (ICT) in character as opposed to planar ICT (PICT). To resolve these long-standing questions, a combined experimental and theoretical study was used to unravel the mechanism of Nile Red's fluorescence. Time-resolved fluorescence measurements indicated that Nile Red emission occurs from a single excited state. Theoretical calculations revealed no evidence for a low-lying TICT state, with the S_1 minimum corresponding to a PICT state. Ultrafast pump-probe spectroscopic data contained no signatures associated with an additional excited state involved in the fluorescence decay of Nile Red. Collectively, these data in polar and nonpolar solvents refute dual fluorescence in Nile Red and definitively demonstrate that emission occurs from a PICT state.



Reproduced from J. Phys. Chem. B 2024, 128, 47, 11768–11775, published by the American Chemical Society under the terms of the **CC-BY-4.0 license**. doi: 10.1021/acs.jpcb.4c06048

Authors: C. Gajo, D. Shchepanovska, J.F. Jones, G. Karras, P. Malakar, G.M. Greetham, O.A. Hawkins, C.J.C. Jordan, **B.F.E. Curchod** ✉, **T.A.A. Oliver** ✉